The Secretion-coupled Endocytosis Correlates with Membrane Tension Changes in RBL 2H3 Cells

Jianwu Dai,* H. Ping Ting-Beall,‡ and Michael P. Sheetz*

From the *Department of Cell Biology and ‡Department of Mechanical Engineering, Duke University Medical Center, Durham, North Carolina 27710

ABSTRACT Stimulated secretion in endocrine cells and neuronal synapses causes a rise in endocytosis rates to recover the added membrane. The endocytic process involves the mechanical deformation of the membrane to produce an invagination. Studies of osmotic swelling effects on endocytosis indicate that the increased surface tension is tightly correlated to a significant decrease of endocytosis. When rat basophilic leukemia (RBL) cells are stimulated to secrete, there is a dramatic drop in the membrane tension and only small changes in membrane bending stiffness. Neither the shape change that normally accompanies secretion nor the binding of ligand without secretion causes a drop in tension. Further, tension decreases within 6 s, preceding shape change and measurable changes in endocytosis. After secretion stops, tension recovers. On the basis of these results we suggest that the physical parameter of membrane tension is a major regulator of endocytic rate in RBL cells. Low tensions would stimulate endocytosis and high tensions would stall the endocytic machinery.

KEY WORDS: membrane tension • membrane tether • laser tweezers • secretion • endocytosis

INTRODUCTION

Stimulation of secretion in neurons or other secretory cells is normally followed by an increase in the endocytosis rate. The rationale for the rise in endocytosis is to recover the secreted membrane, but the basis for the change is unclear. In some cases, endocytosis is extremely rapid after a release, raising the possibility that endocytosis might be physically regulated (Thomas et al., 1994). Such a physical coupling between membrane tension and endocytosis has been observed for plant cells (Kell and Glaser, 1993) and hypothesized for animal cells (Sheetz and Dai, 1996). In these studies we have examined the relationship between endocytosis rates and tension in the plasma membrane for rat basophilic leukemia (RBL)[1] cells following stimulated secretion and hypotonic swelling.

Mechanical regulation of enzymatic function is widely accepted in muscle contraction since myosin's ATPase activity is affected by high tension (Pybus and Tregear, 1975; Smith et al., 1995). However, mechanical regulation could affect other systems such as endocytosis. The formation of an endocytic vesicle requires considerable force to bend the membrane, to displace membrane-associated skeletal components, and to overcome the membrane tension. Therefore, these factors all could act to inhibit the mechanical steps in the endocytic process. As the endocytic machinery draws in membrane, bending stiffness would remain constant as would the association with the cytoskeleton, whereas the membrane tension must rapidly increase as the membrane is drawn down over the cytoskeleton. In spherical plant protoplasts, it has been shown that a mechanical tension in the membrane can regulate the plasma membrane area through alterations in both exo- and endocytosis rates. Changes in osmotic strength will alter plant spheroplast volume such that exocytosis will increase with hypotonic solutions while endocytosis will increase with hypertonic solutions (Kell and Glaser, 1993; Glaser and Donath, 1988). The similar observations on animal cells and the known effects of mechanical force on the rates of enzymes such as motor ATPases led to the hypothesis that animal cell endo- and exocytosis rates as well as cell morphology and motile activity are regulated by membrane tension (Sheetz and Dai, 1996). In addition, hypoosmotic stress increases neuron volume and membrane exocytosis (Morris et al., 1989; Reuzeau et al., 1995), and cell stretch induces increased secretion (Hagmann et al., 1992).

Because of the fluid nature of cell membranes and their high resistance to surface stretch, membrane tension is continuous over the whole cell. Since animal cells are not smooth spheres like plant protoplasts, particularly neuroendocrine cells, not only a mechanical tension but also the adherence of the membrane to the cytoskeleton contributes to the membrane tension (Sheetz and Dai, 1996). In the past, direct measurement of membrane tension was difficult in animal cells and only through the surface deformation of membrane or the formation of thin membranous threads or tethers with micropipets was membrane tension examined experimentally. However, the micropipet tech-

Address correspondence to Dr. Michael P. Sheetz, Department of Cell Biology, Box 3709, Duke University Medical Center, Durham, NC 27710. Fax: 919-684-8592; E-mail mike_sheetz@cellbio.duke.edu

[1]*Abbreviations used in this paper:* DIC, differential interference contrast; DNP, dinitrophenol; RBL, rat basophilic leukemia.

nique is mainly applicable to cells in suspension. The advent of the laser tweezers provides a very flexible method for estimating the tension of adherent cells by forming membrane tethers with beads attached to the cell surface (Dai and Sheetz, 1995*a*, *b*, *c*; Hochmuth et al., 1996).

To measure the membrane tension from a membrane tether, the laser tweezers are used to produce a force on a bead attached to the plasma membrane of a cell, which pulls the membrane into a tether, away from the cytoskeleton (see Fig. 1 *B* for an example). Both the membrane–cytoskeleton adhesion and membrane in-plane tension will draw the tether membrane back onto the cell, thereby creating a tether force (a force pulling the tether back to the cell) on the bead that can be measured directly with the laser tweezers (Dai and Sheetz, 1995*c*; Sheetz and Dai, 1996). From the fluid behavior of the membrane in tethers, it is inferred that the tether membrane lacks cytoskeletal structures (Berk and Hochmuth, 1992). The mathematical relationship between the tether force and the membrane tension was tested on model lipid bilayer systems (Waugh et al., 1992; Evans and Yeung, 1994). Both membrane bending stiffness and tension contribute to the generation of a tether force (Bo and Waugh, 1989; Hochmuth et al., 1996). When membrane tensions were estimated in living cells, the values were ~1% of the force needed to lyse the membrane. Nonetheless, the forces generated on membranes are large enough to alter enzyme activities (Sheetz and Dai, 1996).

In this study we have examined the relationship between endocytosis rates and tension in the plasma membrane for RBL cells following hypotonic swelling and stimulated secretion. The RBL cell was chosen to study stimulated secretion because the secretion process in this system is very well defined. Cross-linking of IgE-receptors by the binding of dinitrophenylated bovine serum albumin (DNP-BSA) to anti-dinitrophenol (DNP) IgE results in the release of cellular serotonin, histamine, and other chemical mediators of the allergic, asthmatic, and inflammatory responses (Foreman et al., 1993; Spudich, 1994; Holowka and Baird, 1996). Following antigen stimulation, these cells undergo morphological changes that include extensive ruffling of the plasma membrane, fusion of the pergranules with the plasma membrane, and, finally, release of granule constituents (Pfeiffer et al., 1985; Ludowyke et al., 1989).

MATERIALS AND METHODS

Cell Culture

RBL 2H3 cells from Dr. T. Meyer's lab (Duke University) were cultured in cell growth wells which were made by using silicone grease to secure a 10-mm diameter cloning cylinder to a 20 × 20 mm (No. 1) glass coverslip (Dai and Sheetz, 1995*a*). The cells were maintained at 37°C, 5% CO_2 in DMEM (BioWhittaker, Walkersville, MD) supplemented with the following: 15% FBS, 2 mM L-glutamine, and gentamycin (10 μg/ml).

Bead Preparation

To prepare IgG-coated beads, rat IgG (Sigma Chemical Co., St. Louis, MO) was dissolved at a concentration of 2.0 mg/ml in PBS. Then, 50 μl of covaspheres (0.5 mm, Duke Scientific, Palo Alto, CA) was added to 50 μl of the above IgG solution and was incubated at 4°C overnight. The beads were pelleted by centrifugation at 2,000 *g* and 4°C for 10 min. Then the beads were resuspended in 1 mg/ml BSA-PBS solution, rinsed by pelleting and resuspension with MEM medium three times, and resuspended in 100 μl MEM medium. For experiments, the bead solution was diluted 3:100 in medium.

Laser Tweezers Manipulations

Just before the laser trap manipulation, the cloning cylinder was removed and a flow chamber was formed. The IgG-covered latex beads were added to the cells through the flow chamber. The cells were imaged by a video-enhanced differential interference contrast (DIC) microscope (IM-35 microscope; Zeiss, Oberkochen, Germany) with a fiber optic illuminator. The stage was maintained at 38°C using an air current incubator. The laser trap consisted of a polarized beam from an 11 W TEM00-mode near-infrared (1,064 nm) laser (model C-95; CVI Corp., Albuquerque, NM) that was expanded by a 3× beam expander then focused through an 80-mm focal length achromatic lens (Melles Griot, Irvine, CA) into the epifluorescence port of the Zeiss IM-35 microscope.

To form a tether from the RBL cell, an IgG-coated latex bead was held on the cell surface for several seconds, and the bead was pulled away from the cell surface by moving the sample with piezoceramic-driven stage (Wye Creek Instruments, Frederick, MD) at a constant velocity. The laser power which reached the sample in all these experiments was below 200 mW. All the experiments were recorded onto video tapes for later analysis.

Tether Force Measurement and Membrane Tension Calculation

Presently there is no theory that can be used to directly calculate the trapping force for beads. All the forces must be determined empirically, and the forces are commonly calibrated against viscous drag exerted by fluid flow. The force on the bead can be obtained if we know the laser trap stiffness, because the force can be determined as a function of a displacement from the trap center. To measure the trap stiffness, a viscous force is generated by oscillatory motion of the specimen by a piezoceramic-driven stage at a constant velocity. The position of the bead in the trap is tracked using the nanometer-level tracking program to analyze video records of the experiments (Gelles et al., 1988). The viscous force on the bead can be calculated through Stokes' Law. For a bead of radius of r, the drag force can be obtained from Stokes' Law: $F = 6\pi\eta rv$. Here η is the fluid viscosity, and v is the flow rate. The calibration shows a very linear force-displacement relationship for the optical tweezers and the slope of the linear fit gives the trap stiffness (Dai and Sheetz, 1995*a*). If the trap stiffness and the displacement of the particle position from the trap center are known, the force on the trap can be easily calculated. To measure the static tether force, a tether was formed and kept at a constant length. Then the bead position in the trap during tether formation was tracked using the nanometer-scale tracking

program (Gelles et al., 1988). The tether force on the bead was calculated from the calibration of the laser trap. To measure the time course of the tether force, a bead was placed on an RBL 2H3 cell which had been incubated with 0.25 μg/ml anti-DNP IgE and was washed three times with the extracellular buffer. The bead was held on the cell surface for several seconds with the laser tweezers and was pulled out at a constant velocity to form the tether. After the tether was formed (average length was ~15 μm), the bead was held stationary and the DNP-BSA solution was added through the flow cell. The static tether force can be obtained from the calibration of the laser trap and bead position in the laser trap.

We estimated the relative tether diameter by determining the tether intensity through orthogonal scans across the DIC image of the tethers from different cells. The intensity is related to the tether diameter (Schnapp et al., 1988).

The technique of tether formation with laser optical tweezers provides a unique way to measure membrane tension. The membrane tension term of the static tether force (F_0) is complicated for cultured cells because there are two major factors that contribute to the static tether force (F_0): membrane bending stiffness (B) and cell surface tension (T). Since the relationship among B, F_0, and tether radius (r_t) is $B = F \cdot r_t/2\pi$ (Hochmuth et al., 1982), B is assumed to be constant, the tether thickness is inversely related to F_0. The membrane tension can then be estimated directly from F_0 by using the following equation: $F_0 = 2\pi\sqrt{2BTm}$ (modified form Hochmuth et al., 1996).

Cell Treatments

To stimulate the RBL secretion, we incubated the cell with monoclonal anti-DNP IgE (0.25 μg/ml) overnight and washed the cells three times with extracellular buffer (125 mM NaCl, 5 mM KCl, 20 mM Na-HEPES, 1.5 mM $MgCl_2$, 1.5 mM $CaCl_2$, pH 7.4). The cells were stimulated with 1 or 2 μg/ml DNP-BSA (0.1 mg/ml BSA was added in DNP-BSA solution) shortly after washing (Spudich, 1994) (within 15 min). To make Ca^{2+}-free medium and buffer, we added 10 mM EGTA and adjusted pH value to 7.4. To block the DNP-BSA–mediated release with DNP-lysine, RBL cells were first stimulated with DNP-BSA at the concentration of 1 μg/ml. After 5 min, DNP-lysine at a concentration of 10 μM was added to the cells, and the cells were incubated at 37°C for 10–15 min.

To measure the time course of cell volume change during cell swelling in hypotonic buffer (50% water/50% medium), RBL cells in suspension were placed in a microchamber with normal medium. A cell was transferred from a microchamber in normal buffer to the microchamber in hypotonic buffer by a glass micropipet (Ting-Beall et al., 1993). The image of the cell during the experiment was digitized and analyzed off line.

Secretion and Endocytosis Measurement

To measure [^{3}H]serotonin release, cells were incubated overnight with [^{3}H]serotonin (2 μCi/ml), washed by aspiration, and then incubated ~5 h in fresh medium containing 0.25 μg/ml anti–DNP-IgE. They were washed immediately before use. [^{3}H]serotonin was measured by liquid scintillation counting in 4 ml EcoLite scintillation cocktail. The total serotonin content was determined from the supernatant radioactivity when 0.5% Triton X-100 was added to the cells. The percentage of [^{3}H]serotonin release was calculated from each condition.

The endocytosis rate of RBL cells is accurately measured by flow cytometry to analyze the intensity of Lucifer yellow dye taken by the cells. Lucifer yellow was dissolved in the medium to a final concentration of 1 mg/ml (pH 7.4). Cells were incubated under different conditions with Lucifer yellow for different times, external dye was washed away, and cells were detached with trypsin-EDTA. Cells were suspended with cold PBS buffer, and the average fluorescence intensity was measured by FACS analyzer. We obtained the signal from fluorescence channel 1 (FL1) and obtained the mean value from 10,000 cells for each sample.

Also, we obtained the information of cell side scattering and forward scattering which relates to cell morphology.

RESULTS

Osmotic Swelling and Shrinkage Modulates Membrane Tension and Membrane Endocytosis Coordinately

In the case of plant spheroplasts subjected to changes in osmotic stress, there was an inverse correlation between membrane tension and the rate of endocytosis. Because the RBL cells might behave similarly, we tested the effects of osmotic swelling and then recovery on membrane tension and endocytosis rate. When transferred to a hypotonic medium, RBL cells rapidly swelled (Fig. 1 *A*).

To follow membrane tension changes, membrane tethers were formed from RBL cells by applying a force with the laser tweezers to a 0.5 micron rat IgG-coated latex bead attached to the plasma membrane. The rat IgG acts like a handle between membrane and the bead. The mechanism of the IgG-coated bead binding to cell surface is not clear. This binding could be nonspecific or specific. Though the aggregation of IgG could activate RBL cells (Benhamou et al., 1994), the rat IgG-coated bead did not cause any effects on the tether force and cell morphology under our experimental conditions. Also, when a ConA-coated bead was used to bind to the cell surface, the tether force was the same as that from rat IgG-coated beads (data not shown). As shown in Fig. 1 *B*, tethers were formed from the side of RBL cells, well away from the glass surface. Video recordings of the bead position were digitally analyzed off-line to obtain the tether force. About 60% of the beads bound to the membrane formed tethers when they were pulled away from the cell by movement of the specimen at a constant velocity with a piezoceramic-driven stage. When the trap was turned off, the beads rapidly (<1 s) returned to the cell surface as the membrane tether was resorbed, indicating that rigid cytoskeletal elements were not part of the tether. During the extension of the tether, the force on the bead included viscous and static components and was very high (Fig. 1 *C*). When the tether was held at constant length to remove the viscous component, the force remained at a value of 22.87 ± 2.96 pN over a measurement period of ~30 s. (Fig. 1 *C*; see Fig. 3 *B*). This tether force was the same for tethers of 10–100 microns in length as was previously observed (Dai and Sheetz, 1995*a*). The tether force was very constant between different cells on different days, and no systematic variation was observed in different regions of the cell surface.

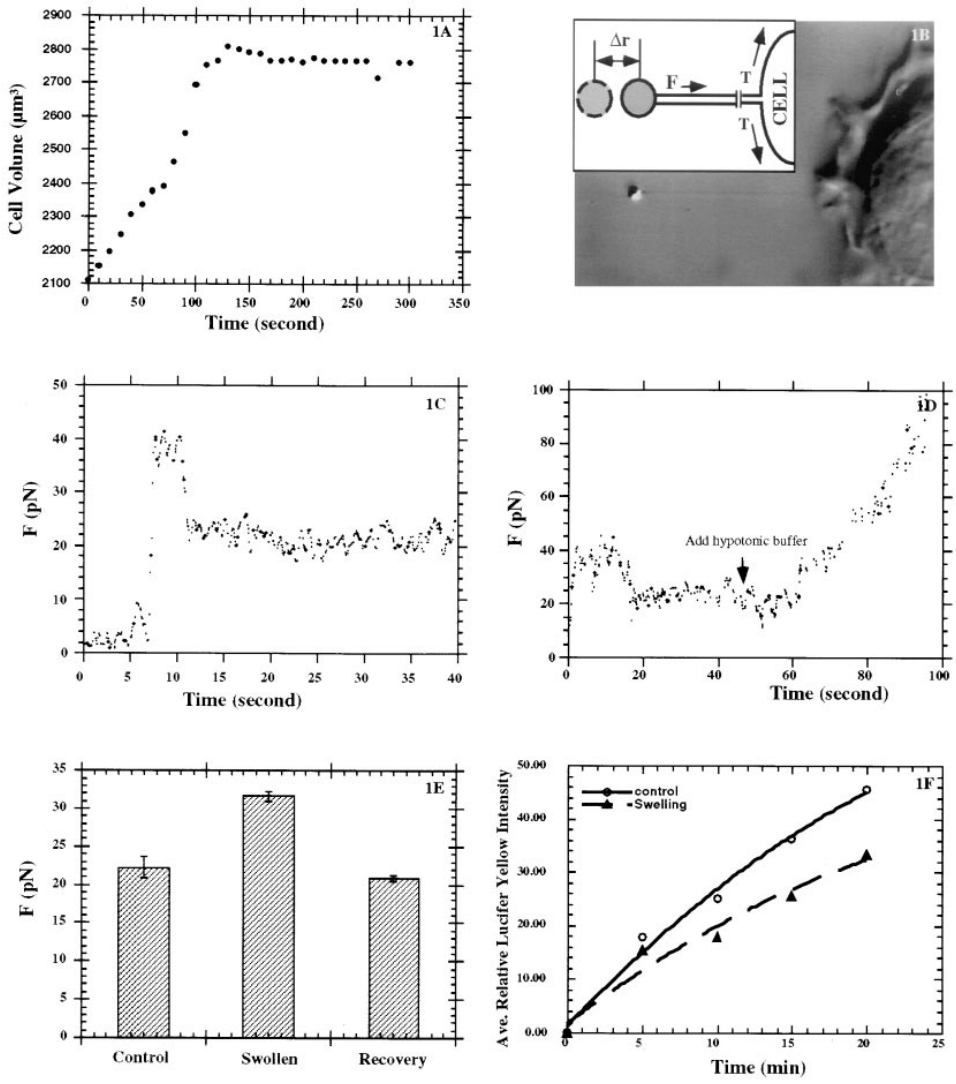

FIGURE 1. (*A*) Time course of RBL cell volume change during cell swelling. An RBL cell was transferred from normal medium to hypotonic buffer (50% water/50% medium) by a micropipet. The cell volume (measured from the cell diameter) increased very fast (within ~2 min) and then stayed constant. (*B*) Photomicrograph of a membrane tension measurement from a RBL cell using a tether. In the diagram, T is the in-plane membrane tension. The tether force (F) can be calculated from the displacement of the bead in the laser trap (Δr) and the calibration of the trap. (*C*) Tether force is plotted versus time and shows elongation and stationary periods. A tether was formed from a control RBL cell. The tether force reached ~39 pN during the elongation period, but it dropped to ~21 pN when held at a constant length. (*D*) Time course of tether force during the RBL cell swelling. A tether was formed and kept at a constant length (before ~40 s), and the hypotonic buffer (50% water/50% medium) was introduced to the cell through the flow chamber (during the time ~44–53 s). The static tether force increased very fast before it reached the limit of the trap strength and the bead escaped from the trap. This time course of tether force is consistent with the time course of cell volume change (*A*) in that the time of most rapid swelling corresponds to the time of highest tether force. (*E*) Average static tether force of swollen RBL cells and after recovery from swollen to isotonicity. The static tether force of swollen cells (31.59 ± 0.63 pN, $n = 15$) is significantly larger than the control cells (22.31 ± 1.41 pN, $n = 17$). The tether force was measured between 5 and 15 min after cells were put into hypotonic buffer. After the swollen cells were transferred to normal isotonic medium, the tether force decreased to 20.78 ± 0.63 pN ($n = 11$) slightly below the control value. The error bars are SEM. (*F*) RBL cell endocytosis rate measured by Lucifer yellow uptake with flow cytometry. The average fluorescence intensity of 10^5 cells was measured as described in MATERIALS AND METHODS. When the cells were incubated with hypotonic buffer, the endocytosis rate was inhibited.

When RBL cells were placed in a hypotonic medium, there was a dramatic increase in tether force to very high levels in the first few minutes (Fig. 1 *D*; we could not trace the tether force all the time during swelling because the trap cannot produce enough force to keep the bead in the trap) followed by a stabilization of the tether force at a level of ~32 pN for the next ~20 min (see Fig. 1 *E* for the swollen cells). If isotonic media was restored after 30 min, the tension dropped dramatically to a value slightly below the control level before ultimately recovering to the control level.

To determine the rate of endocytosis during swelling and shrinking conditions, we used a fluorescence-activated cell sorting (FACS) assay of soluble Lucifer yellow uptake, which showed a linear increase in fluorescence with time (Fig. 1 *F*). When the cells were placed in hypotonic media, there was a significant decrease in the endocytosis rate of swelling cells to about 70% that of the controls (Fig. 1 *F*). Thus, under hypotonic conditions which increase the membrane tension, endocytosis is decreased. After swollen cells were placed in isotonic medium, the membrane tension dropped below control levels, and the endocytosis rate was higher than controls (data not shown).

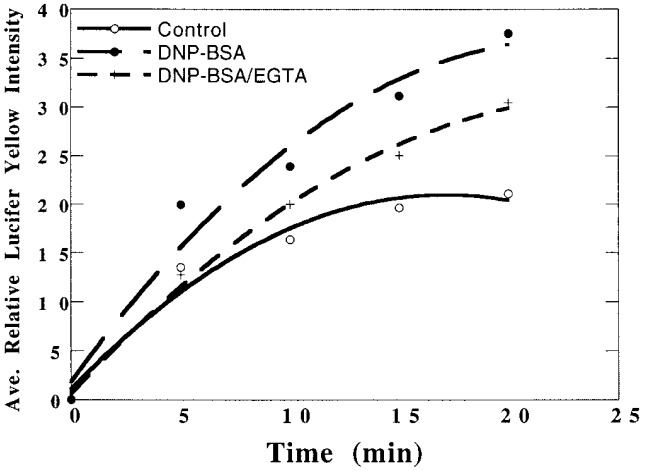

FIGURE 2. RBL cell endocytosis rate is increased upon stimulation of secretion and can be inhibited by removing extracellular Ca^{2+} with EGTA. Endocytosis was measured by FACS analysis for 10^5 cells each sample after Lucifer yellow incubation for control cells or cells treated with 1 μg/ml DNP-BSA or with 1μg/ml DNP-BSA and 10 mM EGTA.

Endocytosis Increased after Stimulated Secretion in RBL Cells

Previous studies had shown that RBL cells would secrete after stimulation with DNP-BSA and that endocytosis would be stimulated. To understand if these RBL cells responded similarly to cross-linking of bound IgE, we measured [^{3}H]serotonin release (Pfeiffer et al., 1985) and Lucifer yellow uptake. Detectable serotonin was released within 30 s after addition of 1 μg/ml DNP-BSA to cells that had been coated with anti–DNP-IgE; and after ~15 min, release was maximal. The release of serotonin was terminated rapidly by addition of an excess of the monovalent, competitive ligand, DNP-lysine (data not shown). This is consistent with the previous reports. An increase in endocytosis after secretion was also observed in RBL cells. Using the FACS assay of Lucifer yellow uptake, there was nearly a threefold increase in endocytosis rate at early times after DNP-BSA stimulated secretion for the adherent cells. This increase of endocytosis can be inhibited by removing extracellular Ca^{2+} by using EGTA (Fig. 2). Thus, these RBL cells secrete normally and respond to secretion by increasing their endocytosis rate.

Membrane Tension Is Decreased in Stimulated RBL Cells

If membrane tension is an important factor in controlling membrane endocytosis rate, then the increase in endocytosis that accompanies stimulated secretion of RBL cells should follow a decrease in membrane tension. When the tether force was measured after stimulation of secretion, a dramatic decrease to 10.58 ± 2.64 pN with 1 μg/ml or 8.40 ± 2.45 pN with 2 μg/ml of DNP-BSA was observed (Fig. 3, *A* and *B*). If secretion was

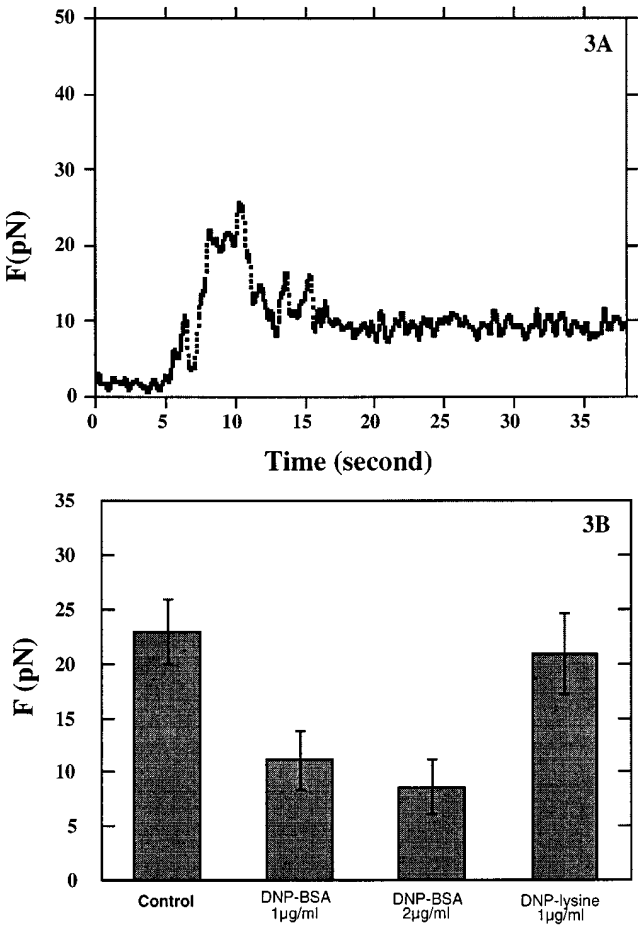

FIGURE 3. (*A*) Tether force during tether formation after stimulation of secretion with DNP-BSA (1 μg/ml). The tether force during the elongation was decreased (~20 pN) compared to control and it decreased further to ~10 pN when held at a constant length (see Fig. 1 *C*, legend). (*B*) The average static tether force for the RBL cells during stimulated secretion. The tether force decreased in cells stimulated to secrete by the addition of 1 and 2 μg/ml DNP-BSA compared to the control cells. There is no substantial difference between the tether forces of nonsecreting cells, when secretion was blocked by DNP-lysine, and the control cells. The error bars are SD.

prevented by removing external Ca^{2+} with EGTA, the tension remained at the control level when 1 μg/ml DNP-BSA was added (22.33 ± 3.30 pN) (see Fig. 6 *B*). Likewise, blocking secretion with DNP-lysine prevented the decrease in tension when DNP-BSA was added (Fig. 3 *B*). Thus, a very significant drop in tether force correlated with secretion.

To determine the time course of the force decrease, we measured the static tether force during stimulation (see Fig. 4 for a representative trace). A tether was formed and held stationary for a short time before 2 μg/ml DNP-BSA was added through a flow cell. The average tether static force decreased from ~24 pN to 12.43 ± 1.56 (n = 4) pN within 10 s after the addition

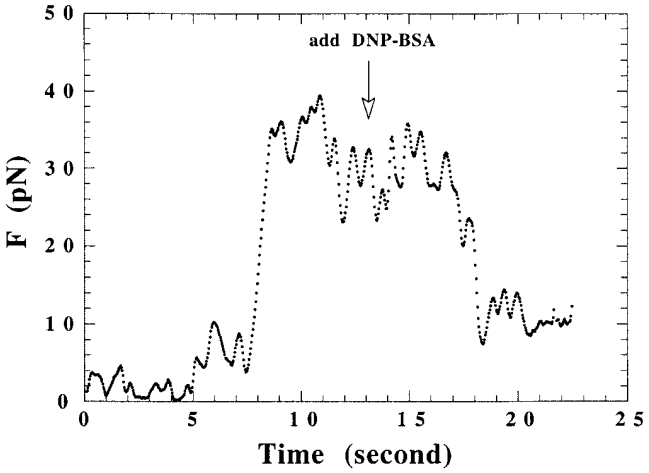

FIGURE 4. Time course of the decrease in tether force during secretion. Extension of the tether started at the time of ~8.5 s and ceased at ~12 s. DNP-BSA (1 μg/ml) was added by flow at the time of ~13 s. The stationary tether force started to decrease at ~19 s, and this meant that the tether force dramatically decreased within 6 s after the addition of the antigen. In four repeats of this experiment, the average tether static force decreased from ~24 pN to 12.43 ± 1.56 (n = 4) pN within 10 s after the addition of DNP-BSA.

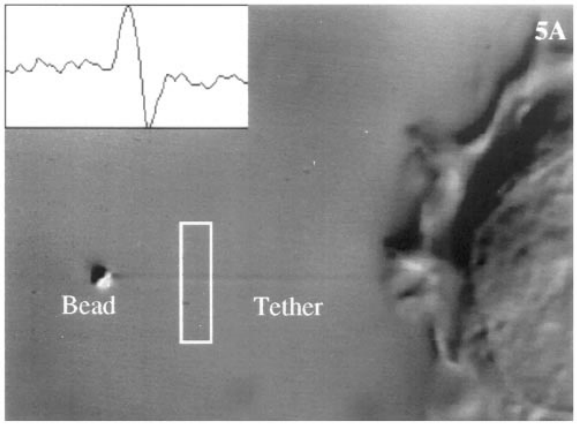

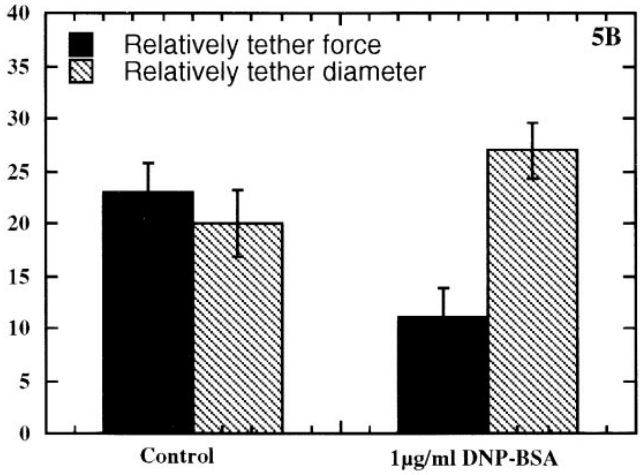

FIGURE 5. (*A*) Photomicrograph showing the method of measuring the relative tether thickness from the DIC image. The intensity of the contrast is related to the tether thickness (Schnapp et al., 1988). The relative tether contrast was determined through integration of changes in intensity along orthogonal scans across the DIC image of the tether. (*B*) The comparison of tether force with the relative tether diameter. For the resting cells (*Control*) and secreting cells (*1 μg/ml DNP-BSA*) the tether force decreased by ~50%, whereas the relative tether diameter increased by ~35%.

of the antigen. In the same experiments, changes in cell morphology such as the formation of projections followed after stimulation of secretion. However, shape changes were not seen for 20–30 s. Thus, the drop in tether force was very rapid and preceded the morphological changes.

From earlier analyses of tether formation, the tether force is dependent upon both the membrane tension and the membrane bending stiffness. To determine if the membrane bending stiffness was significantly altered during secretion, we measured the relative tether diameter from the contrast of the tethers in the DIC image (Schnapp et al., 1988; Hochmuth et al., 1996) (Fig. 5 *A*). In this figure, the trace in the white box is the grey scale scan across the tether image. For a constant bending stiffness, the tether diameter should be inversely related to the membrane tension (Hochmuth et al., 1982, 1996); therefore, the tether diameter should increase upon secretion. We observed that the tether diameter increased by ~35% whereas the force decreased by ~50% (Fig. 5 *B*) in parallel studies on the same day. Using the equations described in MATERIALS AND METHODS, the calculated membrane tension was reduced to 36% of the control upon secretion stimulated with 1 μg/ml DNP-BSA.

Similar Shape Changes Do Not Affect Membrane Tension

During secretion there is a dramatic change in morphology of the RBL cells that is characterized by an increase in actin-rich lamellipodia projections. An antibody, AA4, can cause a similar morphological change without stimulating secretion (Oliver et al., 1992). We have also observed the similar results by scanning electron microscopy (data not shown). When AA4-treated cells were analyzed, no significant change in tether force was observed (data not shown).

Further, when EGTA was used to remove extracellular Ca^{2+} and block stimulated secretion, a dramatic shape change was also observed. Fig. 6 *A* shows the light scattering from cells treated with EGTA, which indicates that in the presence of EGTA, cross-linking IgE receptors with DNP-BSA increases light scattering from cells. Light scattering increases were shown to be caused by cell morphological changes such as membrane ruffling (McNeil et al., 1985). This agrees with

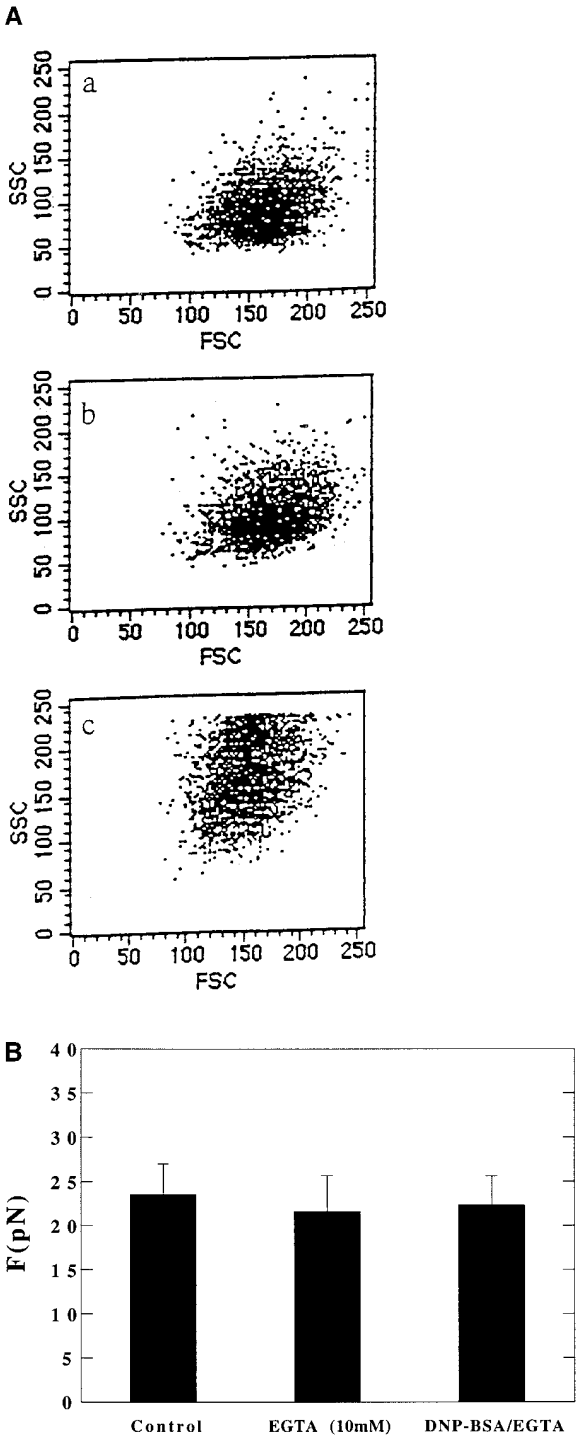

FIGURE 6. (*A*) The cell side scattering (*SSC*) and forward scattering (*FSC*) measured by FACS. All cells were incubated with Lucifer yellow dye for 20 min; (*a*) control, (*b*) cells with 1 μg/ml DNP-BSA, (*c*) cells with 10 mM EGTA and 1 μg/ml DNP-BSA. Cells in *c* have significant increase of SSC which indicates that more dramatic membrane ruffling occurs. (*B*) Membrane tether force was not affected by cell shape changes caused by the treatment with both EGTA and DNP-BSA. The DNP-BSA concentration is 1 μg/ml and EGTA is 10 mM. The error bars are SD.

the observations of cell shape under microscope (data not shown). This shape change is similar to the secreting cells but much more dramatic. When the tether force was measured, it is similar to that of the control cells (Fig. 6 *B*). Thus, cell shape change can occur independently of tether force changes.

DISCUSSION

In these studies, tether force was consistently inversely related to endocytosis rate in RBL cells. Over a nearly fivefold range in tether force, a corresponding inverse change in endocytosis rates of nearly tenfold was observed. Changes in tether force preceded the changes in the cell endocytosis rates when either the cells secreted membrane or experienced changes in medium osmolarity. This is analogous to the plant spheroplasts, where modulating membrane tension above or below 0.1 mN/m results in a corresponding decrease or increase in endocytosis rate. However, plant cells are normally spherical which enables tension to be measured and adjusted by micropipet aspiration. The convoluted nature of the RBL cell surface makes it necessary to utilize the tether force to measure membrane tension (Sheetz and Dai, 1996).

In previous studies of model lipid systems and animal cells, a relationship between tether force and membrane tension was derived. From the model systems, the mechanical tension in a lipid bilayer was shown to be related to the square of the tether force assuming a constant membrane bending stiffness. For a similar relationship to hold in biological membranes, the tethers should not be supported by cytoskeletal elements and should be relatively uniform in composition. Because the tethers retracted rapidly ($<$0.1 s) and showed considerable flexibility, we believe that they contained no cytoskeletal elements as has been found for other tethers (Berk and Hochmuth, 1992). In both the cases of osmotic swelling and stimulated secretion, formed tethers showed changes in tension after addition of hypotonic medium or stimulation of secretion which argues against changes in tether composition. This supports the assumption that membrane bending stiffness is constant since bending stiffness is dependent upon membrane composition. Further, when bending stiffness changes were estimated from the apparent tether diameter changes, only small changes in stiffness were found, particularly when compared to the magnitude of changes in membrane tension. Thus, the changes in tether force with secretion were the result of changes in membrane tension.

In healthy animal cells, the membrane is normally adherent to the cytoskeleton and the two components of the membrane tension, the in-plane tension and the membrane–cytoskeleton adhesion, are not separable (Dai and Sheetz, 1995*c*; Sheetz and Dai, 1996; Hoch-

muth et al., 1996). The other major parameter, membrane bending stiffness, stays relatively constant; therefore, it is clear that the membrane tension term decreases dramatically upon secretion and increases upon swelling. If we assume that the tether force is only from in-plane tension and the bending stiffness is constant at a value of 2.7×10^{-19} N · m (Hochmuth et al., 1996), then we can calculate that the resting in-plane tension would maximally be 0.025 mN/m. During secretion, this drops to about 8 μN/m, but while the cell is in the swollen state, it is high at 48 μN/m. During the swelling phase, we find that the tension exceeds the force of the trap (>500 μN/m); however, even these values are below the tensions needed to produce membrane lysis (~10 mN/m) but may cause opening of stretch-activated channels (2–10 mN/m) (Gustin, 1991).

The tension changes cannot be explained simply as the consequence of addition or deletion of internal membrane to the plasma membrane; because (*a*) a reservoir of membrane exists that buffers tension changes and (*b*) tension jumps between discreet values rapidly. Evidence for a membrane reservoir comes from the fact that increasing tether length from 10 to 100 microns causes no change in tether force (Dai and Sheetz, 1995*a*). For an RBL cell with a surface area of 2,000 μm^2 and a normal elastic coefficient (~600 mN/m), elastic expansion of the plasma membrane by 60 square microns (the membrane area of a 100 micron tether) would cause a 1.8 mN/m rise in tension (Waugh and Evans, 1979), whereas experimentally, there is no change in the 0.02 mN/m resting membrane tension with the formation of a 100 micron tether. Secondly, if the drop in tension with secretion was related to the amount of membrane secreted, then we would expect a more continuous change in the tension with time of secretion. In fact, the decrease from the resting tension to the value of secreting cells occurs within seconds with little time at intermediate values, whereas secretion occurs over minutes. Thus, we suggest that the membrane tension is largely set by the membrane–cytoskeleton interaction and the enzymatic changes associated with secretion could alter the membrane–cytoskeleton interaction.

We find that secretion decreases the membrane tension and that the increase in endocytosis rate can recover the reduced tension. The drop in tether force followed closely the stimulation of secretion and occurred before endocytosis rate changes could be measured. When secretion was blocked by the removal of Ca^{2+} or addition of DNP-lysine, there was no change in tether force. Interestingly, here we found the stimulated endocytosis is Ca^{2+} sensitive, and this is different from the previous report (Pfeiffer et al., 1985). There are two reasonable explanations for this difference: (*a*) the efficiency of removing extracellular Ca^{2+} by EGTA or (*b*) the different effect of Ca^{2+} when cells are in suspension versus adhesion. Our results in this system do show a consistent inverse correlation between membrane tension and endocytosis rate.

IgE alone had no effect on tether force (data not shown), and there was a constant value for the tether force among the control cells. The morphological change that accompanies secretion was also not correlated with the drop in tension since the AA4 antibody could produce a similar alteration in morphology without changing tension significantly, and EGTA and DNP-BSA together cause similar but much more dramatic shape changes which do not change membrane tension. Thus, we suggest that the change in membrane tension correlates with cell secretion and endocytosis rate change and is not because of activation of other pathways such as the shape change, actin dynamics, or membrane activation by receptor cross-linking.

There are other changes that occur in the RBL cells upon secretion, including changes in cell rigidity. In studies of RBL cell cytoskeleton deformation during secretion, the cross-linking of cell-surface IgE-receptors with multivalent ligands caused an increase in the cell or cytoskeletal rigidity (Liu et al., 1987). Membrane tension and cell rigidity are quite different parameters in that the cell rigidity represents the integrated structural characteristics of the cytoskeleton, whereas the membrane tension is a property of the membrane bilayer and its cytoskeletal affinity. It is reasonable to expect that an increase in cell rigidity would cause an increase in membrane tension since cytochalasin B causes a decrease in both cell rigidity and membrane tension. Thus, the effects are clearly separable in the case of secretion.

Previous studies in plant spheroplasts indicate that the response to an increase in membrane tension involves an increase in plasma membrane area, which results from both the decrease in endocytosis and an increase in exocytosis (Kell and Glaser, 1993). Such an area expansion will relieve the tension caused by swelling, and, in the RBL cell, there is also a decrease in endocytosis and an increase in exocytosis (Dai and Sheetz, unpublished results). Plant protoplasts have a smooth spherical surface which makes interpretation of membrane tension simpler than for RBL or other animal cells with complex morphologies (see Sheetz and Dai, 1996). Nevertheless, RBL cells and molluscan neurons (Dai, Sheetz, and Morris, unpublished data) have increased membrane tension upon osmotic swelling and decreased upon shrinking which correlates with the increased exocytosis upon swelling and increased endocytosis upon shrinking. Thus, it appears that osmotic-induced changes in membrane tension alter exocytosis and endocytosis rates in both plant and animal cells in a manner consistent with the hypothesis that tension is a physical regulator of membrane area.

The molecular mechanisms by which changes in membrane tension can be transduced into changes in membrane trafficking are unknown. Endocytosis rates could be regulated physically because of the large forces needed to form endocytic vesicles (Sheetz and Dai, 1996). Both the membrane invagination and the actual budding would be inhibited by membrane tension. For endocytosis, the in-plane tension would resist the early endocytic steps such as membrane invagination and fission. The isotropic nature of the in-plane tension will mean that a force of about 22 pN is required to produce an endocytic pit with an even higher force needed to complete the fission process. Such a force is in excess of forces generated by 10 myosin molecules (Finer et al., 1994).

Regardless of the actual mechanism that is used by cells to regulate the membrane tension, these studies clearly show that the secretion-coupled endocytosis correlates with a decrease in membrane tension and that endocytosis is a way to recover the reduced membrane tension. Endocytosis is a mechanical phenomenon and can be rapidly regulated by mechanical factors which would explain the rapid endocytic response (Thomas et al., 1994). Because the membrane tether force on existing tethers drops rapidly upon the stimulation of secretion and the membrane bending stiffness stays relatively constant, we suggest that a membrane tension decrease causes the tether force decrease. Thus, we favor the hypothesis that membrane tension can regulate plasma membrane surface area through alterations in the rates of endocytosis and exocytosis. Further, we suggest membrane tension is a primary regulator of endocytic rate through its mechanical effect on the proteins responsible for forming the endocytic vesicle.

We thank Dr. T. Meyer for providing the RBL cells and [^{3}H]serotonin; Dr. R.P. Siraganian (Yale University) for kindly providing AA4 monoclonal antibody. We also thank Drs. K. Wang (University of Texas at Austin), R.M. Hochmuth, D. Felsenfeld, C.G. Galbraith, T. Meyer, T. Macintosh, and members in Sheetz's Lab for helpful comments on this manuscript.

This work was supported by grants from NIH, MDA, and HFSP.

Original version received 16 October 1996 and accepted version received 15 April 1997.

REFERENCES

Benhamou, M., E.H. Berenstein, M. Jouvin, and R.P. Siraganian. 1994. The receptor with high affinity for IgE on rat mast cells is a functional receptor for rat IgG2a. *Mol. Immunol.* 31:1089–1097.

Berk, D.A., and R.M. Hochmuth. 1992. Lateral mobility of integral proteins in red blood cell tethers. *Biophys. J.* 61:9–18.

Bo, L., and R.E. Waugh. 1989. Determination of bilayer membrane bending stiffness by tether formation from giant, thin-walled vesicles. *Biophys. J.* 55:509–517.

Dai, J., and M.P. Sheetz. 1995*a*. Mechanical properties of neuronal growth cone membranes studied by tether formation with laser optical tweezers. *Biophys. J.* 68:988–996.

Dai, J., and M.P. Sheetz. 1995*b*. Axon membrane flows from the growth cone to the cell body. *Cell.* 83:693–701.

Dai, J., and M.P. Sheetz. 1995*c*. Regulation of endocytosis, exocytosis and shape by membrane tension. *In* Protein Kinesis: Dynamics of Protein Trafficking and Stability. Coldspring Harbor Laboratory Press, Coldspring Harbor, NY. 567–571.

Evans, E.A., and A. Yeung. 1994. Hidden dynamics in rapid changes of bilayer shape. *Chem. Phys. Lipids.* 73:39–56.

Finer, J.T., R.M. Simmons, and J.A. Spudich. 1994. Single myosin molecule mechanics: piconewton forces and nanometer steps. *Nature (Lond.).* 368:113–119.

Foreman, J.C., J.L. Mongar, and B.D. Gomperts. 1973. Calcium ionophores and movement of calcium ions following the physiological stimulus to a secretory process. *Nature (Lond.).* 245:249–251.

Gelles, J., B.J. Schnapp, and M. P. Sheetz. 1988. Tracking kinesin-driven movements with nanometer-scale precision. *Nature (Lond.).* 331:450–453.

Glaser, A., and E. Donath. 1988. Osmotically-induced vesicle-membrane fusion in plant protoplasts. *Studia Biophysica.* 127:129–138.

Gustin, M.C. 1991. Single-channel mechanosensitive currents. *Science (Wash. DC).* 253:800.

Hagmann, J., D. Dagan, and M.M. Burger. 1992. Release of endosomal content induced by plasma membrane tension: video image intensification time lapse analysis. *Exp. Cell Res.* 198:298–304.

Hochmuth, R.M., J. Shao, J. Dai, and M.P. Sheetz. 1996. Deformation and flow of membrane into tethers extracted from neuronal growth cones. *Biophys. J.* 70:358–369.

Hochmuth, RM., H.C. Wiles, E.A. Evans, and J.T. McCown. 1982. Extensional flow of erythrocyte membrane from cell body to elastic tether. II. Experiment. *Biophys. J.* 39:83–89.

Holowka, D., and B. Baird. 1996. Antigen-mediated IgE receptor aggregation and signaling: a window on cell surface structure and dynamics. *Annu. Rev. Biophys. Biomol. Struct.* 25:79–162.

Kell, A., and R.W. Glaser. 1993. On the mechanical and dynamic properties of plant cell membranes: their role in growth, direct gene transfer and protoplast fusion. *J. Theor. Biol.* 160:41–62.

Liu, Z.Y., J.I. Young, and E.L. Elson. 1987. Rat basophilic leukemia cells stiffen when they secrete. *J. Cell Biol.* 105:2933–2943.

Ludowyke, R.I., I. Peleg, M.A. Beaven, and R.S. Adelstein. 1989. Antigen-induced secretion of histamine and the phosphorylation of myosin by protein kinase C in rat basophilic leukemia cells. *J. Biol. Chem.* 264:12492–12501.

McNeil, P.L., A.L. Kennedy, A.S. Waggoner, D.L. Taylor, and R.F. Murphy. 1985. Light-scattering changes during chemotactic stimulation of human neutrophils: kinetics followed by flow cytometry. *Cytometry.* 6:7–12.

Morris, C.E., B. Williams, and W.J. Sigurdson. 1989. Osmotically-induced volume changes in isolated cells of a pond snail. *Comp. Biochem. Physiol.* 92A:497–483.

Oliver, C., N. Sahara, S. Kitani, A.R. Robbins, L.M. Mertz, and R.P. Siraganian. 1992. Binding of monoclonal antibody AA4 to gangliosides on rat basophilic leukemia cells produces changes to those seen with Fc epsilon receptor activation. *J. Cell Biol.* 116: 635–646.

Pfeiffer, J.R., J.C. Seagrave, B.H. Davis, G.G. Deanin, and J.M. Ol-

iver. 1985. Membrane and cytoskeletal changes associated with IgE-mediated serotonin release from rat basophilic leukemia cells. *J. Cell Biol.* 101:2145–2155.

Pybus, J., and R.T. Tregear. 1975. The relationship of adenosine triphosphatase activity to tension and power output of insect flight muscle. *J. Physiol. (Lond.).* 247:71–89.

Reuzeau, C., L.R. Mills, J.A. Harris, and C.E. Morris. 1995. Discrete and reversible vacuole-like dilations induced by osmo-mechanical perturbations of neurons. *J. Membr. Biol.* 145:33–47.

Schnapp, B.J., J. Gelles, and M.P. Sheetz. 1988. Nanometer-scale measurements using video light microscope. *Cell Motil. Cytoskel.* 10:47–53.

Sheetz, M.P., and J. Dai. 1996. Modulation of membrane dynamics and cell motility by membrane tension. *Trends Cell Biol.* 6:85–89.

Smith, P.G., T. Tokui, and M. Ikebe. 1995. Mechanical strain increases contractile enzyme activity in cultured airway smooth muscle cells. *Am. J. Physiol.* 268:L999–L1005.

Spudich, A. 1994. Myosin reorganization in activated RBL cell correlates temporally with stimulated secretion. *Cell Motil. Cytoskel.* 29:345–353.

Thomas, P., A.K. Lee, J.G. Wong, and W. Almers. 1994. A triggered mechanism retrieves membrane in seconds after Ca(2+)-stimulated exocytosis in single pituitary cells. *J. Cell Biol.* 124:667–675.

Ting-Beall, H.P., D. Needham, and R.M. Hochmuth. 1993. Volume and osmotic properties of human neutrophils. *Blood.* 81:2774–2780.

Waugh, R.E., and E.A. Evans. 1979. Thermoelasticity of red blood cell membrane. *Biophys. J.* 26:115–132.

Waugh, R.E., J. Song, S. Svetina, and B. Zeks. 1992. Local and nonlocal curvature elasticity in bilayer membrane by tether formation from lecithin vesicles. *Biophys. J.* 61:974–982.